Exact quantum, quasiclassical, and semiclassical reaction probabilities for the collinear $F+D_2 \rightarrow FD+D$ reaction*

George C. Schatz,† Joel M. Bowman,‡ and Aron Kuppermann

Arthur Amos Noyes Laboratory of Chemical Physics,§ California Institute of Technology, Pasadena, California 91125

(Received 22 October 1974)

Exact quantum, quasiclassical, and semiclassical reaction probabilities and rate constants for the collinear reaction $F+D_2 \rightarrow FD+D$ are presented. In all calculations, a high degree of population inversion is predicted with P^R_{03} and P^R_{04} being the dominant reaction probabilities. In analogy with the $F+H_2$ reaction (preceding paper), the exact quantum 0→3 and 0→4 probabilities show markedly different energy dependence with P^R_{03} having a much smaller effective threshold energy ($E_T = 0.014$ eV) than P^R_{04} (0.055 eV). The corresponding quasiclassical forward probabilities P^R_{03} and P^R_{04} are in poor agreement with the exact quantum ones, while their quasiclassical reverse and semiclassical counterparts provide much better approximations to the exact results. Similar comparisons are also made in the analysis of the corresponding EQ, QCF, QCR, and USC rate constants. An information theoretic analysis of the EQ and QCF reaction probabilities indicates nonlinear surprisal behavior as well as a significant isotope dependence. Additional quantum results at higher energies are presented and discussed in terms of threshold behavior and resonances. Exact quantum reaction probabilities for the related $F+HD \rightarrow FH+D$ and $F+DH \rightarrow FD+H$ reactions are given and an attempt to explain the observed isotope effects is made.

I. INTRODUCTION

In the preceding paper[1] (hereafter referred to as I), we compared the exact quantum (EQ), quasiclassical forward (QCF), quasiclassical reverse (QCR), and uniform semiclassical (USC) reaction probabilities for the collinear $F+H_2 \rightarrow FH+H$ reaction. The results of all four methods agreed in their prediction of a high degree of population inversion in the products of this exothermic reaction. However, the QCF probabilities were found to differ substantially from the corresponding EQ results in threshold behavior and energy dependence. This could have important consequences regarding the validity of the standard three-dimensional quasiclassical method which has been used on $F+H_2$ (D_2) and which is the three dimensional version of the QCF method. We found much better agreement between the exact quantum probabilities and both the quasiclassical reverse and the uniform semiclassical results, thus indicating that either of the last two methods might be preferred to the quasiclassical forward one in three-dimensional calculations.

In this paper we present the analogous EQ, QCF, QCR, and USC results for the collinear $F+D_2$ reaction over roughly the same range of translational energies as was used in I. We shall also make an analysis of the surprisal function for the EQ and QCF results for $F+D_2$ (and $F+H_2$) to determine if an information theoretic description of the product state distributions can be useful. In addition, exact quantum probabilities for the reactions $F+HD$ (DH) $\rightarrow FH(FD)+H(D)$ are given. We also study the importance of tunnelling and resonances in $F+D_2$. $F+HD$, and $F+DH$. These calculations were done in order to assess the effect of isotopic substitution on the magnitude of the quantum effects and on the validity of the approximate methods.

The potential energy surface used in these calculations is identical to that described in I.[2] In addition, most of the numerical techniques are the same as was used in I and will not be described again here except to note changes made.

In Sec. II we discuss the EQ, QCF, QCR, and USC reaction probabilities for $F+D_2$, and the corresponding collinear rate constants are presented in Sec. III. Section IV contains a study of the behavior of the reaction probabilities at energies sufficiently high to excite the first two vibrational states of reagent D_2. In addition, we discuss resonances in this reaction, giving specific comparisons between the results of the exact quantum, and approximate methods in the vicinity of these resonances. Section V contains a description of the EQ reaction probabilities for $F+HD$ (DH), and in Sec. VI we present a summary of conclusions.

II. QUANTUM, QUASICLASSICAL, AND SEMICLASSICAL REACTION PROBABILITIES FOR COLLINEAR $F+D_2 \rightarrow FD+D$

A. Exact quantum reaction probabilities

Since the vibrational spacing in D_2 is roughly 9 kcal/mole and that in FD is about 8 kcal/mole, and the reaction is exothermic by 32 kcal/mole approximately, at least five vibrational levels of DF are accessible when D_2 has an initial quantum number $v=0$. By coincidence, the $v=3$ and 4 vibrational levels of DF have nearly the same total energies as the $v=2$ and 3 vibrational levels of HF, respectively. This results in remarkable similarities between these two reactions despite the significant difference in the corresponding reduced masses ($\mu_{F,H_2}/\mu_{F,D_2} = 0.548$). As in I, we will designate by $P^R_{vv'}$ the reaction probability for a reagent initially in state v to form product in state v', and by P^R_v the total reaction probability from initial state v (i.e., $\sum_{v'} P^R_{vv'}$). In Fig. 1 we present the exact quantum reaction probabilities P^R_{04}, P^R_{03}, and P^R_0 for $F+D_2$ at relative translational energies (E_0) in the range 0.0–0.25 eV. The corresponding probabilities P^R_{02}, P^R_{01}, and P^R_{00} are plotted in Fig. 2. It is apparent from these figures that P^R_{04} and P^R_{03} are the most significant contributors to P^R_0 in this E_0 range. The P^R_{02}, P^R_{01}, and P^R_{00} curves are all very similar in appearance to the P^R_{03} one, but with greatly

reduced magnitudes ($P_{02}^R \sim 6.8\times10^{-2}\ P_{03}^R$, $P_{01}^R \sim 5\times10^{-4}\ P_{03}^R$, $P_{00}^R \sim 6\times10^{-6}\ P_{03}^R$). There is a very significant difference between the threshold behavior of P_{03}^R and that of P_{04}^R quite analogous to what was observed in I for the reaction probabilities P_{02}^R and P_{03}^R of F + H_2. As in I, it is convenient to define an effective threshold energy E_T for the $v \to v'$ reaction as the difference between the (lowest) energy for which the corresponding $P_{vv'}^R$ is equal, say, to 1% of the maximum value attained by this quantity and the energy at which the $v \to v'$ process becomes energetically possible. Table I contains the values of E_T for several important reaction probabilities for the reactions of F with H_2, D_2, HD, and DH as well as the corresponding vibrationally adiabatic zero curvature barrier heights E_{VAZC} (described in I). From it we see that for F + D_2 the value of E_T for P_{03}^R (EQ), 0.014 eV, is appreciably lower than the E_{VAZC} value of 0.032 eV. This can be interpreted as an indication of the extent of vibrationally adiabatic one-dimensional tunnelling (see paper I) in this system. The value of E_T for P_{03}^R (QCF) of 0.030 eV is very close to E_{VAZC}. This suggests that the chemical motion for this system is nearly vibrationally adiabatic in the approach coordinate in the sense that the local action number for the motion transverse to the reaction coordinate should vary relatively little between the separated reagent region and the saddle point region. The corresponding values of E_T and E_{VAZC} for P_{02}^R (EQ) of F + H_2 are 0.005 eV and 0.026 eV,

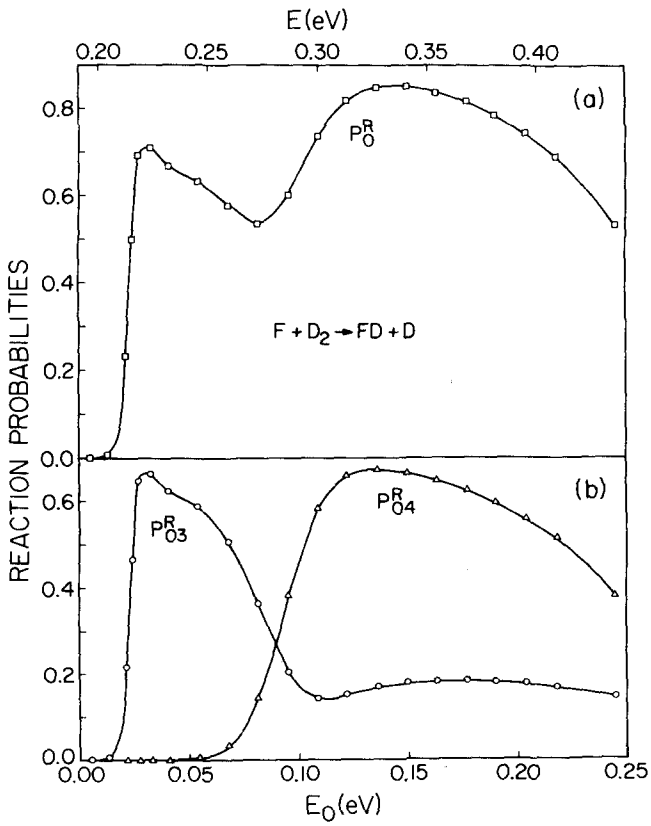

FIG. 1. Exact quantum reaction probabilities for F + D_2 as a function of relative translational energy E_0 and total energy E (relative to minimum in D_2 diatomic potential curve). (a) Total reaction probability P_0^R. (b) Reaction probabilities P_{03}^R and P_{04}^R.

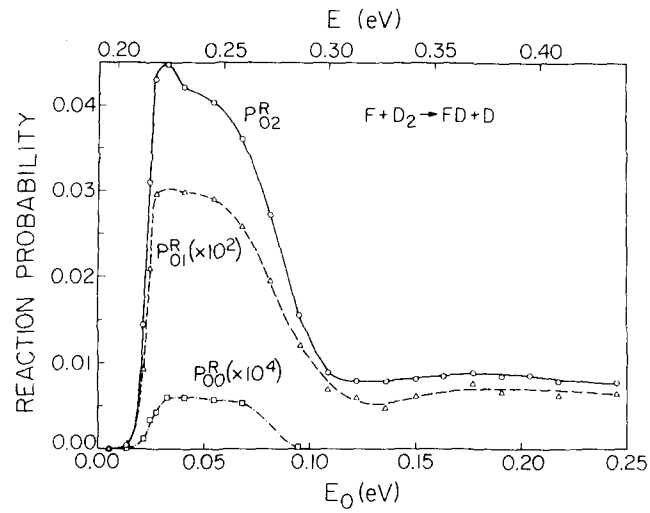

FIG. 2. Exact quantum reaction probabilities P_{02}^R, P_{01}^R, and P_{00}^R for F + D_2 (similar to Fig. 1).

indicating somewhat more tunnelling in this system than in F + D_2, as expected. The effective threshold energy of P_{04}^R (F + H_2) (E_T = 0.055 eV) is similar to that of P_{03}^R (F + H_2) (0.045 eV). The near coincidence in energy between the v = 3 and 4 vibrational levels of FD and v = 2 and 3 of FH is probably responsible for the very similar appearance of the corresponding EQ reaction probabiliti ities. (Compare Fig. 2 of I with Fig. 1 of the present paper.) There are, however, differences in the maximum values of certain analogous reaction probabilities, especially P_{03}^R (F + D_2) and P_{02}^R (F + H_2) (which have maximum values of 0.66 and 0.44, respectively). We shall see in Sec. IV that the differences between analogous reaction probabilities for the two reactions become even more important for $E_0 > 0.25$ eV.

B. Quasiclassical reaction probabilities

In Fig. 3 are plotted the QCF and EQ reaction probabilities P_{03}^R, P_{04}^R, and P_0^R for F + D_2. No reactive trajectories yield DF with v' = 0 or 1, but there is a small probability of reaction to v' = 2 (always < 0.1 and vanishing for $E_0 > 0.12$ eV). The corresponding QCR reaction

TABLE I. Effective threshold energies (E_T) for the most significant reaction probabilities in the F + H_2, F + D_2, F + DH, and F + HD reactions.[a]

	F + H_2	F + HD
$E_T[P_{02}^R(\text{EQ})]$	0.005	0.010
$E_T[P_{02}^R(\text{QCF})]$	0.025	N.C.[b]
$E_T[P_{03}^R(\text{EQ})]$	0.045	0.071
$E_T[P_{03}^R(\text{QCF})]$	0.012	N.C.[b]
E_{VAZC}	0.026	0.028
	F + D_2	F + DH
$E_T[P_{03}^R(\text{EQ})]$	0.014	0.011
$E_T[P_{03}^R(\text{QCF})]$	0.030	N.C.[b]
$E_T[P_{04}^R(\text{EQ})]$	0.055	0.022
$E_T[P_{04}^R(\text{QCF})]$	0.030	N.C.[b]
E_{VAZC}	0.032	0.028

[a]All energies are in eV.
[b]No QCF calculations were done for this transition.

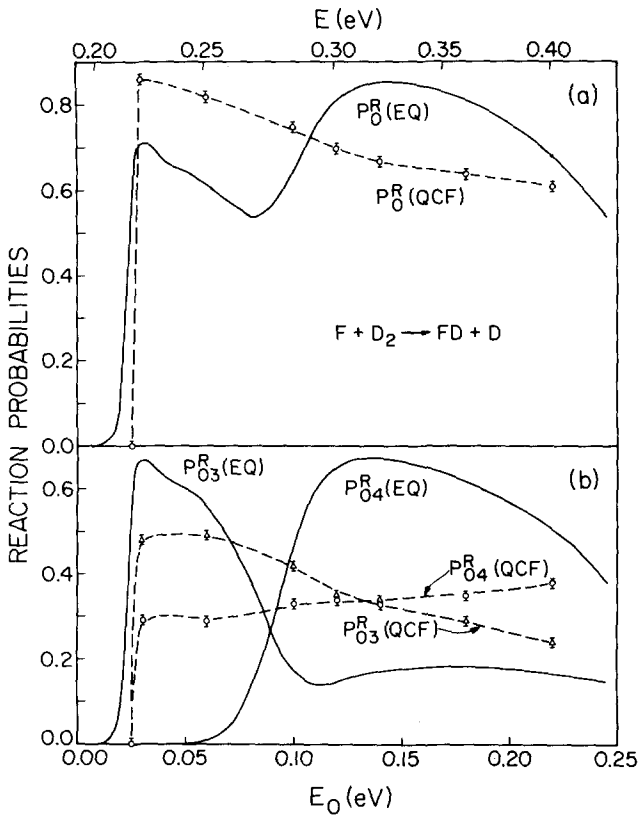

FIG. 3. Quasiclassical forward (dashed curve) and exact quantum (solid curve) reaction probabilities for F + D_2: (a) P_0^R, (b) P_{03}^R and P_{04}^R.

probabilities for the same energy range ($0.0 < E_0 < 0.12$ eV) are plotted in Fig. 4. In Fig. 3 we see that there is a very large difference between the threshold behavior of P_{04}^R (EQ) and P_{04}^R(QCF). In analogy with the F + H_2 P_{03}^R behavior,[1] we find that the quasiclassical reverse P_{04}^R of F + D_2 (Fig. 4) has a threshold behavior which is much closer to the exact quantum one than is the QCF threshold. Unlike P_{02}^R (F + H_2), the energy dependence of P_{03}^R (F + D_2) is predicted somewhat more accurately by the QCF method than by the QCR method. The EQ and QCF total reaction probabilities P_0^R (Fig. 3) are in somewhat better average agreement than are the EQ and QCF total reaction probabilities in F + H_2 (Fig. 4 of Paper I). This seems to indicate that the differences between quantum and classical dynamics are less severe for F + D_2 than for F + H_2. However, at least for collinear reactions, these differences are still quite significant.

In Fig. 5 we plot as a function of E_0 the fraction f_v of the total energy which appears as vibrational energy of the DF product for the EQ and QCF calculations. It can be seen that f_v (QCF) is nearly independent of E_0 and has an average value of 0.79. The corresponding EQ curve has a more pronounced E_0 dependence but about the same average value over the E_0 range considered. We find that the average value of f_v is almost the same for both F + H_2 and F + D_2. This independence of isotopic substitution agrees with the corresponding experimental result[2] and with the predictions of three-dimensional trajectory calculations,[3] although our value of f_v(0.79) which ignores rotational degrees of freedom is somewhat higher than the experimental result (0.66).[4] This general average agreement between the EQ and QCF f_v vs E_0 curves indicates that the dynamic processes governing the *average* energy disposal between vibrational and translational degrees of freedom of the products can be well approximated by the classical trajectory method. However, one should keep in mind that this is not so for the distribution of this vibrational energy among the available vibrational states, i.e., that large differences between product state population ratios obtained from the EQ and QCF methods do exist, as indicated in Fig. 6.

C. Semiclassical reaction probabilities

Figure 7 shows the uniform semiclassical reaction probabilities P_{03}^R and P_{04}^R along with the corresponding EQ results. The USC results are similar to the ones obtained independently by Whitlock and Muckerman in an analogous calculation.[20] It was noted in Paper I (Sec. III C) that "raggedness" (i.e., very rapid variation of m_f with q_0) in the final action number m_f (q_0; v, E) as a function of initial vibrational phase q_0 caused difficulties in calculating USC transition probabilities at the threshold of the F + H_2(0) → FH(3) + (H) reaction. The same problem occurred for the 0 → 4 transition in the F + D_2 reaction, and was also encountered by Whitlock and Muckerman. We were able to overcome this difficulty by using the reverse final action number function, $n(q_0; m, E)$, which was found to be smooth for $m = 4$ and n around 0. The justification for using this procedure was given in I.

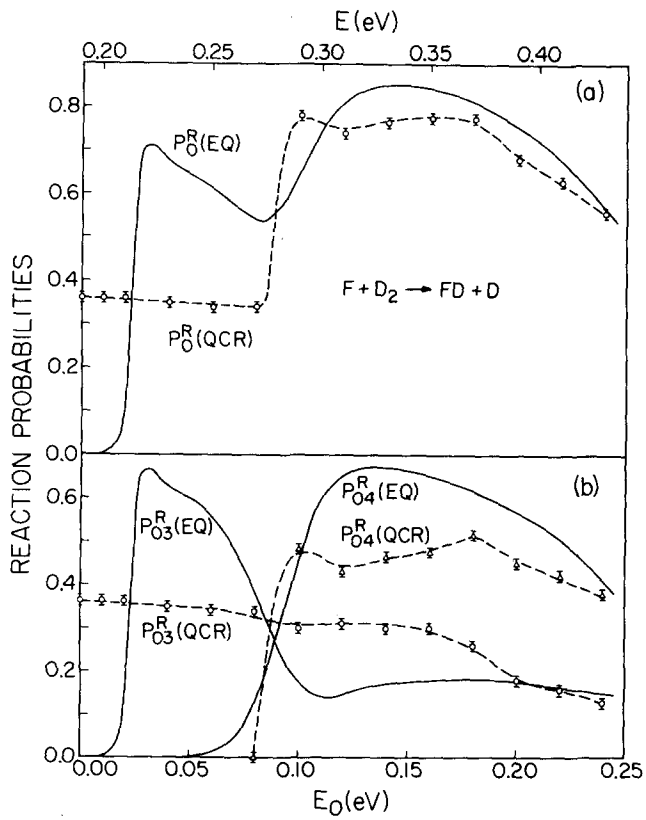

FIG. 4. Quasiclassical reverse (dashed curve) and exact quantum (solid curve) reaction probabilities for F + D_2: (a) P_0^R, (b) P_{03}^R and P_{04}^R.

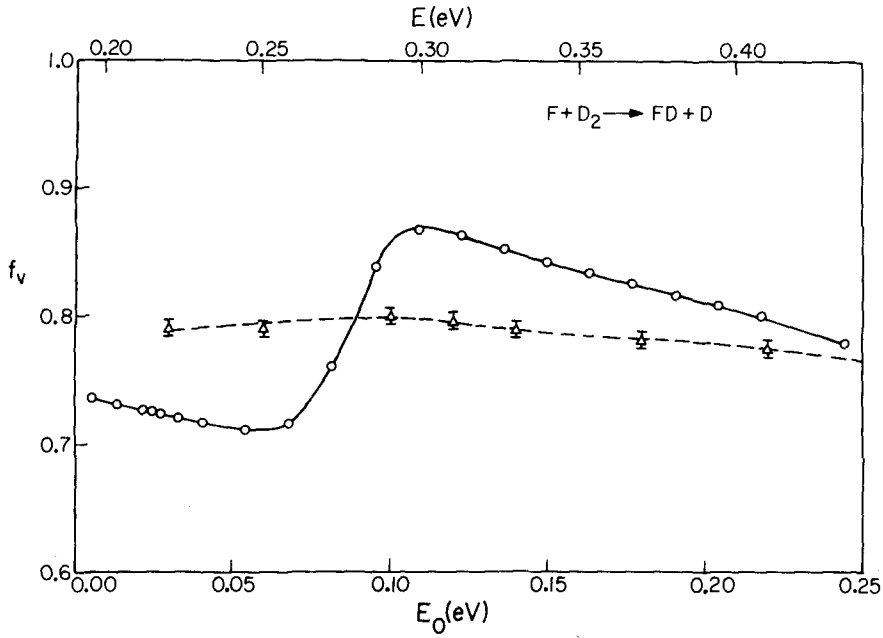

FIG. 5. Fraction (f_v) of the total reagent energy (exclusive of product zero point energy) which ends up as vibrational energy in the product DF plotted as a function of the reagent translational energy E_0 and total energy E. Solid line indicates EQ results and dashed line QCF ones. Other notation analogous to Fig. 1.

The curves for the forward and reverse values of m_f for this 0 → 4 transition at an energy $E = 0.3107$ eV ($E_0 = 0.12$ eV) are given in Fig. 8. When all the relevant semiclassical quantities are well-behaved ("nonragged") functions of q_0, the USC transition probabilities obey microscopic reversibility,[5] and it is not necessary to calculate both the forward and reverse results. However, as the example above demonstrates, when raggedness exists, it is advisable to consider the forward and the reverse results. In our example, the reverse results are the preferred ones, since there is no raggedness in the region corresponding to D + DF(4) → D_2(0) + F. These were the ones used in calculating P_{04}^R (and P_{03}^R for the F + H_2 reaction) in its threshold region. The USC P_{04}^R transition probabilities at $E_0 = 0.08$ eV and 0.085 eV were calculated in the statistical approximation.[6] At these energies the reverse reaction showed that the 4 → 0 transition was dynamically forbidden. However, since statistical (i.e., ragged) behavior was evident in the forward reaction, we did calculate a nonzero value for P_{04}^R at the two energies just mentioned.

The USC probabilities in Fig. 7 are in much better agreement with the corresponding EQ results than are the quasiclassical ones. As was the case with the QCF P_{03}^R threshold, there is a small difference between the P_{03}^R (USC) and P_{03}^R (EQ) threshold energies, but the USC result may be improved by using complex trajectories.[7]

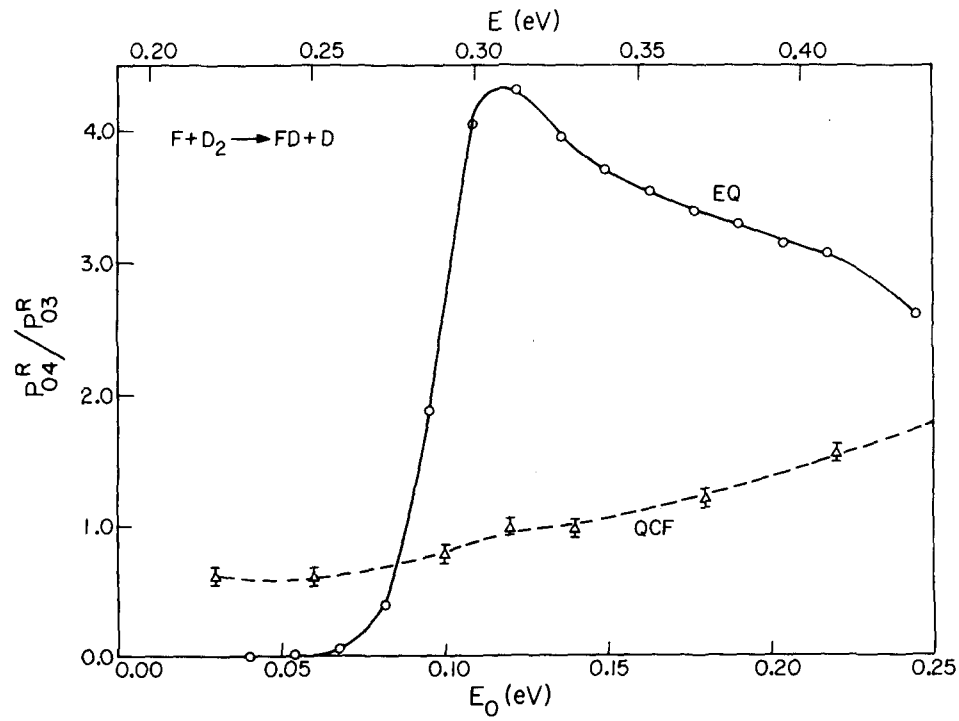

FIG. 6. Ratio of reaction probabilities P_{04}^R/P_{03}^R vs translational energy E_0 and total energy E. Solid line indicates EQ results and dashed line QCF ones. Other notation analogous to Fig. 1.

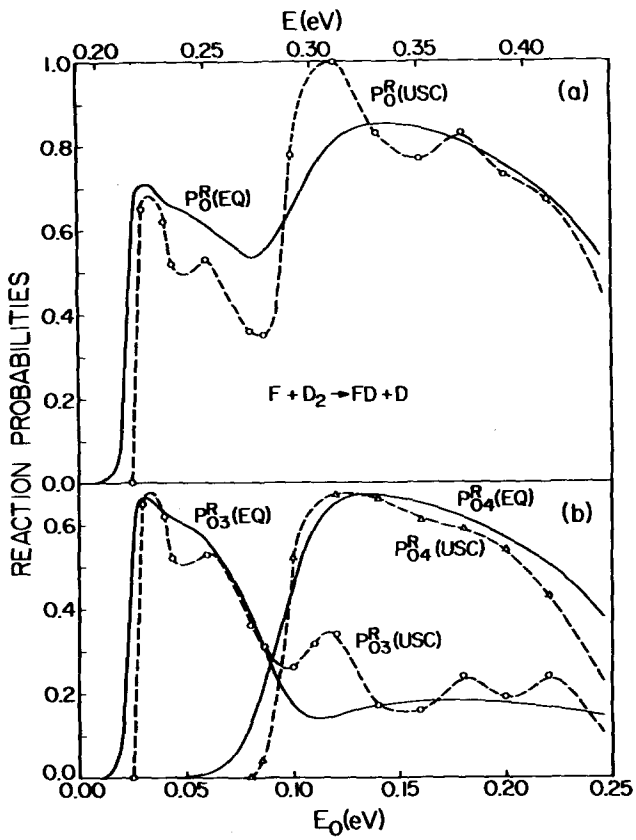

FIG. 7. Uniform semiclassical (dashed curve) and exact quantum (solid curve) reaction probabilities for F + D_2: (a) P_0^R, (b) P_{03}^R and P_{04}^R.

The oscillations in P_{03}^R (USC) in the E_0 range 0.10 eV–0.25 eV do not have any analog in the quantum results. These oscillations are due to phase interferences arising from a relatively rapid variation with energy of the differences in phases associated with the two contributing trajectories. One might expect that the raggedness in the plot of final action vs initial phase [see Fig. 8(a)] could be an indication of resonant behavior in this energy range, but the quantum results of Fig. 1 do not substantiate this. In Sec. IV we discuss the possible relationship between resonances in the EQ results and raggedness in the USC ones.

One significant aspect of the comparison between the USC and EQ results in Fig. 7 is that the maximum values of the EQ and USC reaction probabilities P_{03}^R and P_{04}^R are nearly identical. This contrasts with the results of both the QCF and QCR calculations which generally tend to underestimate the maximum values of the probabilities (Figs. 3 and 4). The significant improvement in the quality of the results obtained in going from the quasiclassical to the semiclassical approximation suggests that an equivalent improvement may occur for the three-dimensional F + D_2 reaction and that the semiclassical results may be quite reliable for this case. However, we must stress that the utilization of uniform rather than primitive semiclassical techniques is essential to the success of this method for the collinear reaction, and thus it seems likely that an analogous uniform procedure will be required in the three-dimensional problem.[8]

D. Comparison of EQ, QCF, QCR, and USC reaction probabilities

In Fig. 9 we compare the reaction probabilities P_{03}^R and P_{04}^R of F + D_2 as calculated by all four methods EQ, QCF, QCR, and USC. Figure 10 presents the analogous comparison for the total reaction probability P_0^R. It is apparent from both figures that the USC method gives the best agreement with the EQ reaction probabilities for this reaction.

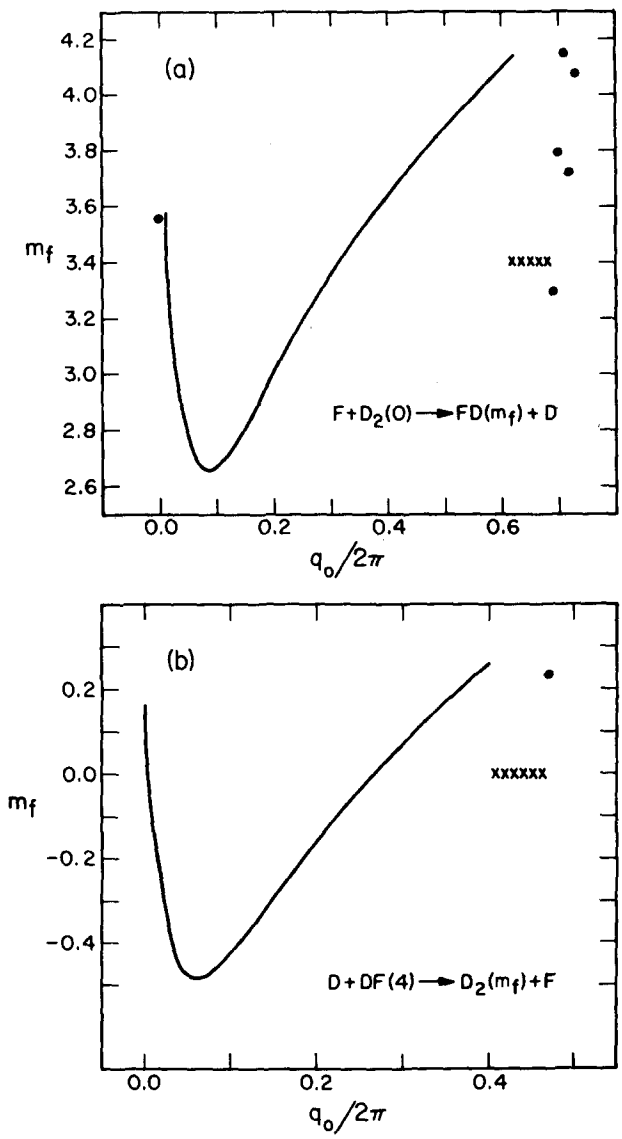

FIG. 8. (a) m_f vs q_0 for the forward F + D_2 (0) → FD(m_f) + D, at a total energy E of 0.3107 eV; (b) m_f vs q_0 for the reverse reaction D + DF(4) → D_2(m_f) + F, at the same total energy E. The solid curves represent the majority of the reactive trajectories computed. The dots and crosses represent, respectively, reactive and nonreactive trajectories in regions of raggedness, for which m_f varies very rapidly with q_0. Since the values of m_f for nonreactive trajectories correspond to a different range of variation than the reactive ones, the crosses were placed at an arbitrary ordinate and are only meant to indicate the values of q_0 for which such trajectories occur.

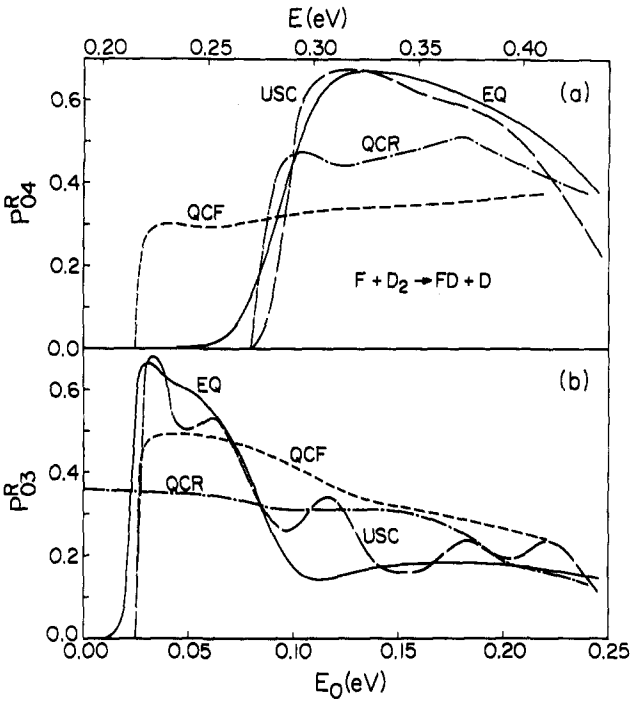

FIG. 9. EQ (solid), QCF (short dash), QCR (dash–dot), and USC (long dash) reaction probabilities P^R_{04} (a) and P^R_{03}(b). (From Figs. 1, 3–4, 7.)

E. Information-theoretic analysis of EQ and QCF reaction probabilities

It is also of interest to perform an information–theoretic analysis of the EQ and QCF results. In this section, we shall consider both the F + D_2 reaction probabilities discussed above and the F + H_2 probabilities described in Paper I.

In analogy with the equations used in three-dimensional studies,[9] we have used a one-dimensional form of the surprisal for a vibrational distribution given by

$$I(f_{v'}) = -\ln[P(f_{v'})/P^0(f_{v'})].$$

$P(f_{v'})$ is the normalized reaction probability to product vibrational state v' expressed as a function of the fraction of the total energy which becomes vibrational energy in the product DF or HF (exclusive of product zero point energy). $P^0(f_{v'})$ is the statistical reaction probability to state v' and is given by

$$P^0(f_{v'}) = \frac{(1-f_{v'})^{-1/2}}{\sum_{v'=0}^{v'^*}(1-f_{v'})^{-1/2}},$$

where the sum is over all accessible product vibrational states. Note that this expression for $P^0(f_{v'})$ predicts inverted statistical vibrational population distributions. This rather surprising result for such a distribution is a straightforward consequence of the use of a one-dimensional density of states function [which varies as $(E_{v'})^{-1/2}$, where $E_{v'}$ is the translational energy relative to vibrational state v'] rather than the corresponding three-dimensional density (which varies as $E_{v'}^{1/2}$).

Figure 11 depicts the EQ and QCF surprisal functions $I(f_{v'})$ vs $f_{v'}$ for F + D_2 and F + H_2 at three different relative translational energies. We see that none of the EQ or QCF plots has the straight line dependence on $f_{v'}$ required if the distribution is to be characterized by a single information–theoretic temperature parameter. The most severe deviations of the EQ results from linearity occur at the lowest energies and are a direct consequence of the unusual threshold behavior of P^R_{04} in F + D_2 and P^R_{03} in F + H_2. This threshold effect is not present in the QCF results, and yet the surprisal functions associated with these probabilities show strong deviations from linearlity. The curves in Fig. 11 indicate that at least in this case, the information–theoretic analysis has limited usefulness as a predictive tool for estimating unknown reaction probabilities from known ones. For example, if we assumed a linear surprisal function and used the results of the two largest EQ probabilities to predict the third largest by linear extrapolation, we would be in error by at least 1 order of magnitude in most of the examples depicted in Fig. 11.

Figure 11 also indicates that in many situations, the surprisal function is not independent of isotopic substitution. This is especially true of the EQ results with $v' = 0$, 1, where the differences between the surprisal functions for F + D_2 and F + H_2 are quite large. However, at higher energies [Fig. 11(a), especially] and for higher vibrational quantum numbers ($v' = 2$–4), the EQ points for both F + D_2 and F + H_2 fall on essentially the same curve. In addition, the QCF results for F + D_2 and F + H_2 in both Figs. 11(a) and 11(b) seem to form a single curve, and for this reason, only one dashed line was drawn through the points. This indicates that at certain energies and for certain ranges of $f_{v'}$, the surprisal function is independent of isotopic substitution, but this property is not generally valid.

The behavior of the surprisal functions (nonlinearity and dependence on isotopic substitution) observed in these collinear results contrasts strongly with the shape of the corresponding surprisal functions obtained from three-dimensional trajectory calculations and experiments on the same reactions.[9] In the three-dimensional case, linear surprisal functions which are nearly inde-

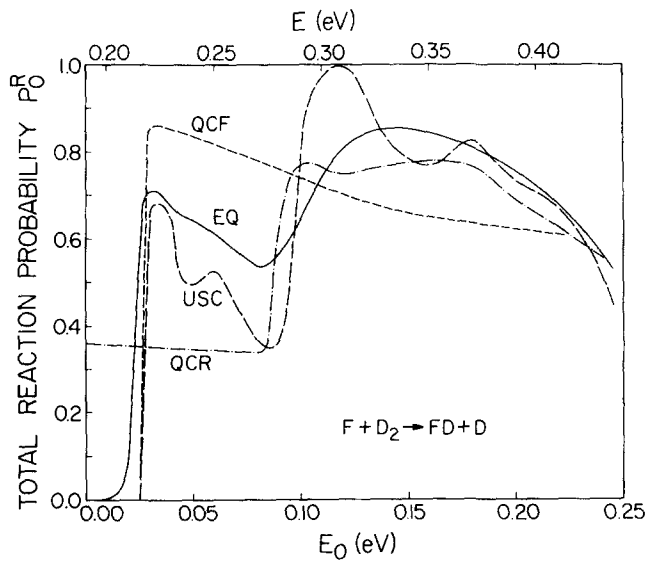

FIG. 10. EQ (solid), QCF (short dash), QCR (dash–dot), and USC (long dash) total reaction probabilities P^R_0 for F + D_2. (From Figs. 1, 3–4, 7.)

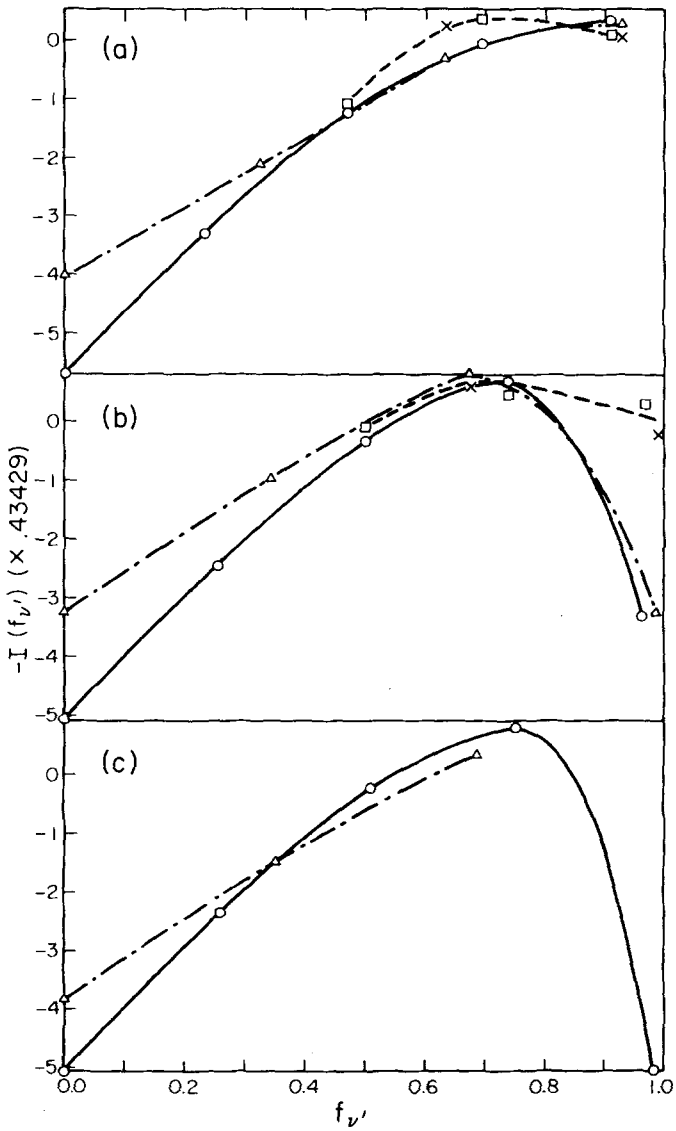

FIG. 11. Surprisal function $I(f_{v'})$ vs fraction $f_{v'}$ of the total product energy which is in product vibrational state v' (exclusive of zero point energy). Symbols plotted have the following meanings: circles—EQ results for F + D_2; triangles—EQ results for F + H_2; squares—QCF results for F + D_2; and crosses—QCF results for F + H_2. (a) $E_0 = 0.12$ eV, (b) $E_0 = 0.03$ eV, (c) $E_0 = 0.005$ eV. The F + D_2 (EQ) results are connected by a solid line, while a dashed–dotted line connects the F + H_2 (EQ) results. A dashed line approximately connects both F + H_2 and F + D_2 (QCF) results. Note that at the lowest energy considered [Fig. 10(c)], only $v' = 0$–2 of HF are energetically accessible, and all QCF reaction probabilities are zero.

pendent of isotopic substitution were obtained in an analysis of the detailed rate constants (rather than reaction probabilities) from both quasiclassical trajectory calculations and from infrared chemiluminescence experiments (which are, of course, quantum mechanical). We have analyzed the surprisal functions for our collinear EQ rate constants for both F + H_2 and F + D_2 (Sec. III) and find no marked change from the results depicted in Fig. 11, the nonlinearity and dependence on isotopic substitution being essentially as pronounced as for the reaction probabilities.

Recently, the relationship between the one- and three-dimensional classical surprisal functions was computationally investigated,[10a] and it was proposed[10b] that the surprisal function should be approximately dimensionally invariant. Our comparison of the one- and three-dimensional surprisal functions for F + H_2 and F + D_2 indicates that this dimensional invariance does not hold for these reactions. Although the validity of our conclusion depends in part on the accuracy of the potential energy surface used in our calculations, we would not expect it to be qualitatively changed if a more accurate potential energy surface were used. In addition, we note that three-dimensional quasiclassical results for F + H_2 and F + D_2 on similar approximate surfaces[3] agree with experiment in their prediction of a linear surprisal function.[9] The computational comparison of one- and three-dimensional surprisal functions of Ref. 10a involved several model potential energy surfaces, but none of these similated the attractive nature of the F + H_2 interaction. We conclude that the invariance of the surprisal function with respect to the dimensionality of the collision may depend significantly on the characteristics of the potential energy surface being considered. Therefore, caution must be exercised in attempting to obtain 3-D reaction cross sections from collinear reaction probabilities.[10b]

III. EQ, QCF, QCR, AND USC RATE CONSTANTS FOR F + D_2

The rate constants k_{03}^R and k_{04}^R obtained from the EQ, QCF, QCR, and USC reaction probabilities P_{03}^R and P_{04}^R for F + D_2 are plotted in Fig. 12. The expression for these rate constants is the same as the one given in Paper I.[1] The corresponding Arrhenius parameters obtained from fits to the rate constants in the 200–400 K and 900–1200 K temperature ranges are listed in Table II. The difference between k_{04}^R (QCF) and k_{04}^R (EQ) (which results from the different threshold properties of the P_{04}^R's in Fig. 9) is quite noticeable and leads to a 0.8 kcal difference between the corresponding high temperature activation energies in Table II. In analogy with our F + H_2 study,[1] the QCR and USC rate constants k_{04}^R and corresponding activation energies E_{04}^a agree with the EQ ones better than do the QCF quantities. The similar comparison for the rate constants k_{03}^R is much less satisfactory. The low temperature differences between the various k_{03}^R's are determined to a large extent by the different threshold energies of the corresponding reaction probabilities P_{03}^R. The transition probability P_{03}^R (QCR) has zero threshold energy and thus the largest rate constant at low temperatures, while the EQ, USC, and QCF P_{03}^R's have successively higher threshold energies and therefore successively lower rate constants. [See Fig. 9(b).] This illustrates that the low energy (< 0.03 eV) behavior of the reaction probabilities (or cross sections) can be exceedingly important in determining the low temperature (< 300 K) behavior of the corresponding rate constants for these reactions.

The ratios k_{04}^R/k_{03}^R are plotted as a function of temperature in Fig. 13. We see that the QCF ratio is nearly temperature independent while the EQ, QCR, and USC ratios increase monotonically with increasing temperature, approaching the QCF ratio at high temperatures.

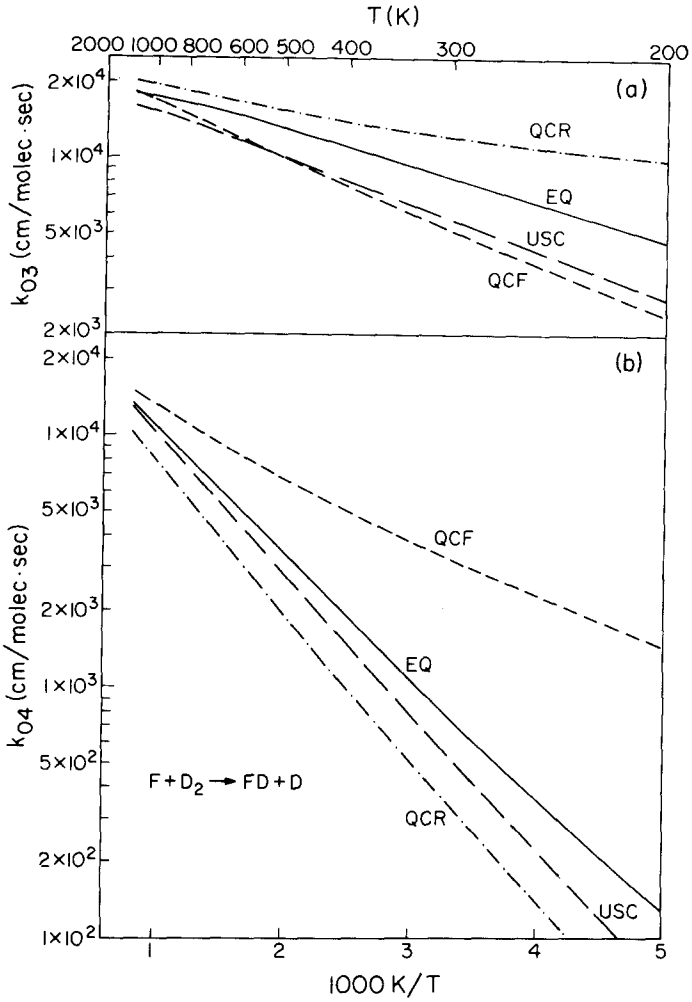

FIG. 12. Arrhenius plot of EQ (solid), QCF (short dash), QCR (dash–dot), and USC (long dash) rate constants for F + D_2: (a) k_{03}^R, (b) k_{04}^R.

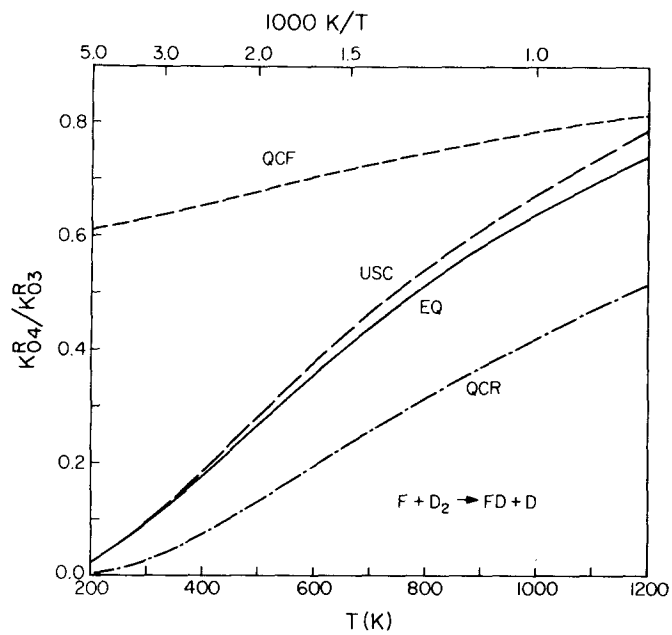

FIG. 13. Ratios of rate constants k_{04}^R/k_{03}^R for F + D_2; EQ (solid), QCF (short dash), QCR (dash–dot), USC (long dash).

These k_{04}^R/k_{03}^R ratios are quite similar in appearance to the k_{03}^R/k_{02}^R ratios for the F + H_2 reaction given in Fig. 12 of Paper I, but the F + D_2 ratios actually increase somewhat more slowly with temperature than do the F + H_2 ones.

The QCF ratio k_{04}^R/k_{03}^R is 0.63 at 300 K, in approximate agreement with the experimental value[11] of 0.66. The results of three-dimensional classical trajectory calculations indicate that this ratio is not strongly temperature dependent.[12] If this is also true experimentally then, in analogy with F + H_2, we would have evidence that the collinear model overestimates the effects of threshold differences on reaction rates to different product vibrational states. We might note, however, that Lee and co-workers[12,13] have measured the ratio of cross sections σ_{04}/σ_{03} at three different energies, and they find that it increases rapidly with increasing energy from 0.75 at $E_0 = 0.034$ eV to 3.5 at $E_0 = 0.11$ eV. If we consider the analogous collinear ratio P_{04}^R/P_{03}^R (Fig. 6), we find that it also increases rapidly with increasing energy (much more rapidly than Lee's cross section ratio) from near zero at zero translational energy to roughly a value of 4.3 for $E_0 \sim 0.12$ eV. The ratios of cross sections from three-dimensional QCF trajectory calculations over a family of several potential energy surfaces do not reproduce this energy dependence (Ref. 12, Table VI). This may indicate that the differences between quantum and quasiclassical results are still significant in three dimensions and, indeed, are observable in experiments which are at least partially state selected such as cross section measurements.

TABLE II. Arrhenius rate constant parameters for F + D_2 → FD + D.[a]

	Temperature range (K)	EQ	QCF	QCR	USC
E_a^{03}	200–400	0.676	0.935	0.266	0.852
E_a^{04}	200–400	2.167	0.990	2.576	2.471
A_{03}	200–400	2.551×10^4	2.443×10^4	1.884×10^4	2.340×10^4
A_{04}	200–400	2.775×10^4	1.686×10^4	2.502×10^4	3.269×10^4
E_a^{03}	900–1200	0.361	0.912	0.416	0.611
E_a^{04}	900–1200	2.108	1.343	2.742	2.344
A_{03}	900–1200	2.104×10^4	2.674×10^4	2.402×10^4	2.082×10^4
A_{04}	900–1200	3.240×10^4	2.604×10^4	3.261×10^4	3.365×10^4

[a] E_a^{0i} is in kcal/mole and A_{0i} is in cm/(molecule·sec).

IV. HIGHER ENERGY REACTION PROBABILITIES FOR F + D_2

Figure 14 shows the higher energy exact quantum reaction probabilities P_{03}^R, P_{04}^R, P_{05}^R, P_{14}^R, and P_{15}^R for F + D_2 in the translational energy range $E_0 = 0.25-0.70$ eV. Those transition probabilities not plotted are all small (usually < 0.02). P_{04}^R (QCR) is also plotted in Fig. 14 in the energy range 0.25–0.42 eV for reasons to be discussed in detail below. This figure is analogous in many ways to Fig. 13 of I, although the close correlation between the reaction probabilities of F + H_2 and the related F + D_2 ones (see end of Sec. II A) becomes less important as the energy is increased. Nevertheless, many of our remarks concerning the F + H_2 reaction probabilities described in I are also applicable here. We note that the transition probabilities P_{15}^R in Fig. 14 and P_{04}^R in Fig. 1 have similar translational energy dependences except near threshold. This confirms our statement in I that reaction probabilities for reagents initially in $v = 1$ are virtually insensitive to the presence of a barrier in the F + H_2 (D_2) reagent channel. In addition, P_{15}^R is significantly larger than the other $P_{1v'}^R$, with $v' < 5$ over the energy range considered. This implies that the additional vibrational energy in the reagents is being predominantly channelled into additional vibrational energy in the products.[14]

The transition probability P_{05}^R exhibits a rather unusual energy dependence. As shown in Fig. 14, it remains quite small (< 0.01), even though energetically allowed, until the total energy becomes high enough to excite $v = 1$ of D_2, at which point it rises suddenly to a peak value of 0.34 before finally levelling off at about 0.13. It is not obvious how simple resonance or threshold theories can explain this unusual behavior, since the effective threshold is apparently related to the opening of a vibrational state not involved in the transition asymptotically. One possible explanation for the influence of the $v = 1$ state of D_2 on this transition probability can be formulated by observing that the inelastic $0 \rightarrow 1$ transition probability for F + D_2 is quite appreciable[15] (0.10–0.25) and, as noted above, P_{15}^R is quite large. This suggests that the $0 \rightarrow 5$ reactive transition occurs almost exclusively with $v = 1$ as an intermediate state. It is also significant that it is not sufficient for this state to be accessible via virtual transitions, rather, it must be open asymptotically. This seems to indicate that a high degree of vibrational excitation must be maintained over a considerable region in configuration space. This would only be possible if the $v = 1$ vibrational state is open, and hence there is no enhancement of P_{05}^R when the state is closed.

For the transitions P_{04}^R at $E_0 = 0.327$ eV and P_{15}^R at $E_0 = 0.599$ eV, we see peaks in the reaction probabilities suggestive of internal excitation resonances.[16] In contrast to the resonances observed in Paper I in F + H_2, the direct processes in F + D_2 still seem to be quite important in the vicinity of the resonances. The resultant interference between the direct and resonant contributions to the scattering amplitude leads to characteristic oscillations in the reaction probabilities in the vicinities of the resonance energies quite similar to what was observed in the H + H_2 reaction.[16,17] As in the F + H_2 reaction, we see an approximate correspondence between the appearance of a resonance and the opening of a specific vibrational state of the product DF ($v = 5$ at $E_0 = 0.29$ eV and $v = 6$ at $E_0 = 0.59$ eV). This implies that the virtual states of the triatomic complex may have energy levels resembling product states more than reagent states. The relation is probably complicated, however, since the correspondence between the resonance energy and the energy of the associated product vibrational level is not always in the same direction (i.e., the resonance energy is sometimes greater and sometimes smaller than the corresponding vibrational energy gy, as can be seen in Fig. 13 of Paper I and Fig. 14 in the present paper).

It is interesting to note that the QCR reaction probability P_{04}^R depicted in Fig. 14 seems to "average out" the quantum oscillations in P_{04}^R (EQ) in the vicinity of the $E_0 = 0.327$ eV resonance. It is also of interest to examine the semiclassical results at this energy. Rankin and Miller have reported extensive statistical behavior in

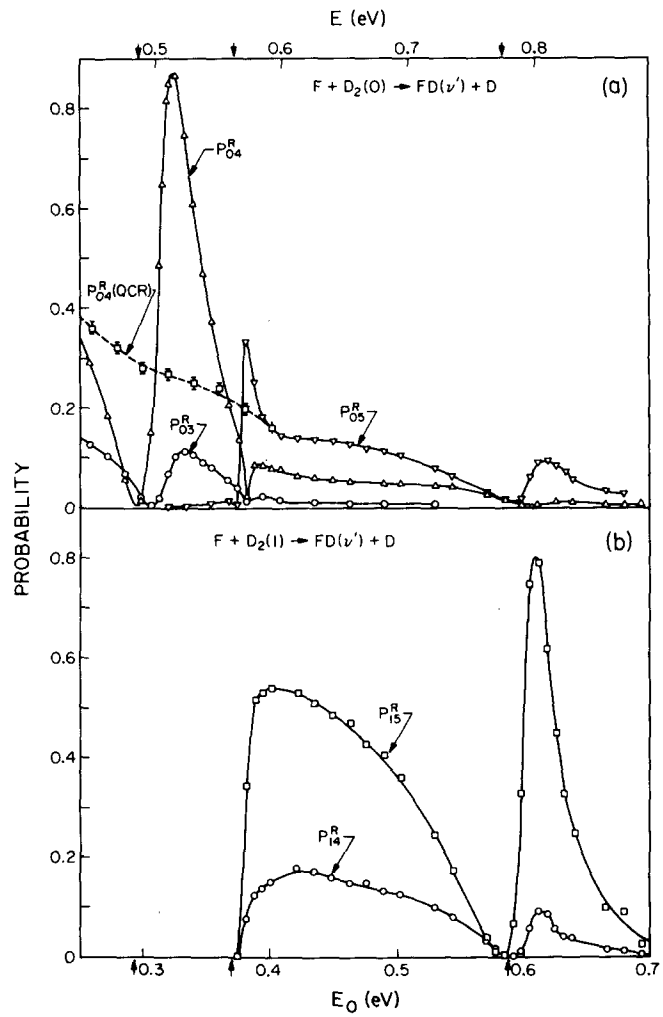

FIG. 14. Exact quantum reaction probabilities at translational energies higher than those in Fig. 1. (a) P_{03}^R, P_{04}^R, and P_{05}^R, (b) P_{14}^R and P_{15}^R. Also shown in (a) is the QCR P_{04}^R curve (dashed). Arrows near $E_0 = 0.29$ eV and 0.59 eV indicate the opening of $v = 5$ and 6, respectively, of DF, while that at 0.37 eV indicates the energy E_0 at which $v = 1$ of D_2 becomes accessible.

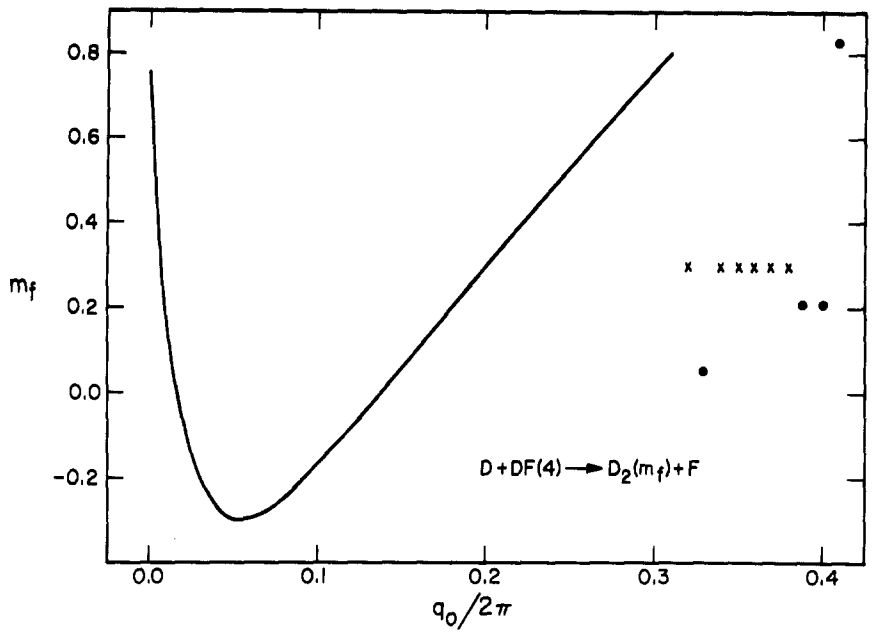

FIG. 15. m_f vs q_0 for the reverse reaction D + DF (4) → $D_2(m_f)$ + F at the resonance nergy 0.5107 eV (corresponding to $E_0 = 0.32$ eV). See Fig. 8 for explanation of dots and crosses.

the final action number function, m_f, for the H + Cl_2 collision.[6] From this behavior, they inferred that a converged quantum treatment of that reaction would yield internal excitation resonances. However, as Fig. 15 shows, m_f, at the resonance energy, is a reasonably smooth function of q_0 with about the same degree of raggedness (i.e., very rapid variation of m_f with q_0) as seen previously away from resonance in Fig. 8(b). An accurate EQ study of the collinear H + H_2 reaction has shown that P_{00}^R has a broad resonance at 0.90 eV total energy and a narrow one at 1.28 eV, and that both are due to interference effects between direct and compound-state mechanisms.[16] Recently, Stine and Marcus[18] searched for and found snarled (i.e., multiple collision) trajectories in the narrow region of q_0 between the reactive and nonreactive branches of the $m_f(q_0; \nu, E)$ curve. They showed that the broad resonance at 0.90 eV could be generated semiclassically if interference effects between direct and snarled trajectories are included, a result consistent with the lifetime analysis of the accurate quantum calculations.[16] Were it not for the knowledge of the existence of this resonance derived from the EQ calculations, it would be easy to miss such snarled trajectories in a semiclassical calculation in which the density of the q_0 grid was not high enough.[5,19] Inclusion of a search of these trajectories and of their effects on the reaction probabilities significantly increases the computational effort involved in the semiclassical approach. Narrow resonances, such as the one occurring at 1.28 eV in collinear H + H_2, may be even more difficult to calculate semiclassically, since its long lifetime[16] suggests that it may correspond to extremely snarled trajectories, requiring inclusion of multiple collisions of high order[18] and use of an extremely high density q_0 grid. In the present paper, we have only included the effect of direct (i.e., nonsnarled) trajectories in the semiclassical calculations. It would be interesting to add the effect of snarled ones, in order to verify whether they could reproduce the resonant behavior of P_{04}^R at $E_0 = 0.327$ eV.

We conclude that raggedness in the $m_f(q_0; \nu, E)$ curves could perhaps be a necessary condition for the existence of quantum mechanical internal excitation resonances, but it is certainly not a sufficient one, as shown by the presence of raggedness in Fig. 8(b), calculated at a nonresonant energy.

V. EXACT QUANTUM REACTION PROBABILITIES FOR THE REACTIONS F + HD → FH + D AND F + DH → FD + H

We have also calculated the exact quantum reaction probabilities for F + HD → FH + D and F + DH → FD + H, hereafter designated F + HD and F + DH, respectively. In three dimensions, these two reactions represent different product arrangement channels of the same collision system. In collinear collisions, however, they must be considered entirely separately. This implies that coupling between these two product arrangement channels is ignored in our collinear calculations.

The largest reaction probabilities for the two reactions are plotted in Fig. 16[20] as a function of the reagent translational energy E_0 (relative to $\nu = 0$ of HD) in the range 0–0.25 eV. For F + HD, the only reaction probability greater than 0.025 in the energy range studied is P_{02}^R, while P_{04}^R, P_{03}^R, and P_{02}^R are the major contributors to the total reaction probability in F + DH (P_{02}^R is always less than 0.10). From Fig. 16 it is apparent that the reaction probabilities P_{04}^R and P_{03}^R of F + DH are very similar in shape to the corresponding probabilities P_{04}^R and P_{03}^R of F + D_2 (Fig. 10), although the sharp differences between the threshold energies of P_{04}^R and P_{03}^R (F + D_2) are reduced considerably for P_{04}^R and P_{03}^R (F + DH). In contrast, the results for F + HD do not show a strong resemblance to those for F + H_2 (Fig. 2 of Paper I). Instead, we see that P_{02}^R (Fig. 16) consists of one very sharp (width ~0.0005 eV) spike near 0.012 eV and then

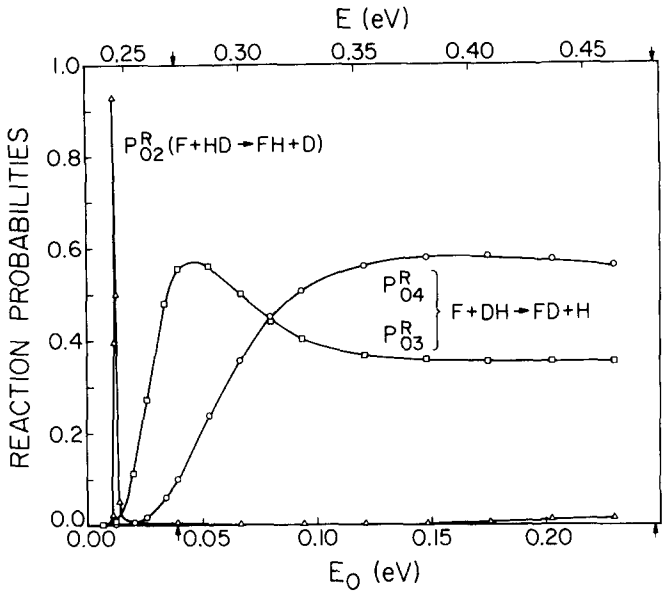

FIG. 16. Exact quantum reaction probabilities P^R_{02} for F + HD, and P^R_{03} and P^R_{04} for F + DH as a function of relative translational energy E_0 and total energy E (relative to minimum in HD diatomic potential curve). Arrow near 0.04 eV indicates the energy at which $v = 3$ of HF becomes accessible.

remains quite small (< 0.02) for the remainder of the energy range studied. P^R_{03}, which is energetically forbidden until $E_0 = 0.039$ eV, is quite small throughout the energy range considered here. The rather dramatic differences between the results for F + HD and F + DH can probably be explained as resulting from the difference in the mass of the atom being exchanged in the collinear triatomic collision system. The small mass of the H atom in F + HD in comparison with that of the D atom in F + DH results in much more important pseudocentrifugal barriers in "turning the corner" in the former reaction than in the latter. That this should be the case is apparent from a comparison of the skew angles (defined in Paper I) for these two systems. For F + HD this angle is 37.3°, while for F + DH it is 56.7°, thus indicating that the curvature along the reaction path should be much larger for F + HD than for F + DH. Only at low translational energies do the centrifugal effects become small enough to render F + HD dynamically allowed. For F + DH, on the other hand, the centrifugal effects are not important in the energy range studied, and thus we observed very large reaction probabilities throughout that energy range.

From Fig. 16, we can also conclude that the rate constant for formation of DF is predicted to be greater than that for formation of HF [except at very low temperatures (< 150°), where the slightly smaller effective threshold of F + HD becomes important]. This disagrees with the experimental result[21] that the rate of H atom transfer is a factor of 1.45 faster than that for D atom transfer at 298 K. The disagreement can probably be explained by noting that the distance of the H atom from the center of mass of HD is about twice that of the D atom from the same center of mass. This means that H sweeps through a larger volume of space than D when HD rotates and thus is more "visible" to the attacking F atom. Since the barrier height is quite low (except near the "perpendicular" orientation[12]), one would expect that H should be preferentially abstracted. For collinear reactions, this three-dimensional effect is ignored and we find, instead, that dynamical effects such as pseudocentrifugal barriers are important in the reaction. These centrifugal effects favor reaction with the D atom and thus explain why the collinear results differ from the experimental ones. A similar argument has been used to explain the J dependence of three-dimensional quasiclassical cross sections for the same reactions.[3a] One might add that for a reaction with a high barrier, which simultaneously favors reaction through collinear geometries, the three-dimensional effect should be less important and the collinear results should be more representative of the experimental results. This has indeed been observed for the Cl + HD (DH) reactions.[22]

VI. DISCUSSION

We shall now summarize the differences between the results of the exact quantum, quasiclassical, and semiclassical methods for studying the F + H_2 (Paper I) and F + D_2 reactions. The most important of these differences may be categorized into three divisions: vibrationally adiabatic tunnelling, resonances, and threshold dynamical effects. These effects may, however, be coupled to one another to a lesser or greater extent.

Vibrationally adiabatic tunnelling seems to be most significant at very low energies, especially for F + H_2 and for those transitions for which at threshold there are no strongly restrictive dynamical effects (of the type occurring in P^R_{03} for F + H_2). Such tunnelling appears to be responsible for important differences between EQ and QCF rate constants at low temperatures [Figs. 11(a) in I and also 12(a) in this paper]. The semiclassical complex trajectory method (which was not studied here) may be able to describe tunnelling quantitatively.[5,7] Internal excitation resonances seem to be very important at higher translational energies and will therefore not be significant in thermal experiments. They may be important in beam and hot atom experiments if these resonance effects carry over without strong attenuation into three dimensions.[23] The current semiclassical theories do not seem to furnish a computationally practical description of the interference effects associated with these resonances.[20] Threshold dynamical effects are very significant for collinear F + H_2 and F + D_2, and this leads to important differences between exact quantum and quasiclassical reaction probabilities and rate constants for thermal distributions of reagents. These threshold effects are partially classical in nature, since we found that the QCR method was capable of describing roughly the proper threshold behavior within a completely classical framework. An important result of this paper was the demonstration that the uniform semiclassical method provides a greatly improved description of threshold behavior of the quantum results in comparison with the QCF method. How important these threshold effects will be in three dimensions is not entirely clear from an analysis of existing experimental and theoretical studies, but it appears that the effects

are at least partially attenuated by the averaging that inevitably occurs in experimental measurements. They may, however, still be important for experiments which are sufficiently state selected.

ACKNOWLEDGMENTS

We thank J. T. Muckerman, with whom we have exchanged results on the USC calculations, for useful discussions. We also thank Ambassador College for the use of their computational facilities in most of the work reported here.

*Work supported in part by the United States Air Force Office of Scientific Research.

†Work performed in partial fulfillment of the requirements for the Ph. D. degree in Chemistry at the California Institute of Technology.

‡Present address: Department of Chemistry, Illinois Institute of Technology, Chicago, IL 60616.

§Contribution No. 4989.

[1]G. C. Schatz, J. M. Bowman, and A. Kuppermann, J. Chem. Phys. 63, 674 (1975), preceding paper.

[2](a) J. T. Muckerman (private communication); (b) P. A. Whitlock and J. T. Muckerman, J. Chem. Phys. 61, 4618 (1974).

[3](a) J. T. Muckerman, J. Chem. Phys. 54, 1155 (1971); (b) *ibid.* 56, 2997 (1972).

[4]J. C. Polanyi and K. B. Woodall, J. Chem. Phys. 57, 1574 (1972).

[5]J. M. Bowman and A. Kuppermann, J. Chem. Phys. 59, 6524 (1973).

[6]C. C. Rankin and W. H. Miller, J. Chem. Phys. 55, 3150 (1971).

[7]W. H. Miller and T. F. George, J. Chem. Phys. 56, 5668 (1972); J. D. Doll, T. F. George, and W. H. Miller, J. Chem. Phys. 58, 1343 (1973); J. Stine and R. A. Marcus, Chem. Phys. Lett. 15, 536 (1972).

[8]W. H. Miller, J. Chem. Phys. 54, 5388 (1971); R. A. Marcus, J. Chem. Phys. 57, 4903 (1972); J. D. Doll and W. H. Miller, J. Chem. Phys. 57, 5019 (1972); J. N. L. Connor, Mol. Phys. 25, 181 (1973).

[9](a) A. Ben-Shaul, R. D. Levine, and R. B. Bernstein, Chem. Phys. Lett. 15, 160 (1972); (b) A. Ben-Shaul and R. D. Levine, J. Chem. Phys. 57, 5427 (1972).

[10](a) C. Rebick, R. D. Levine, and R. B. Bernstein, J. Chem. Phys. 60, 4977 (1974); (b) R. B. Bernstein and R. D. Levine, preprint.

[11]M. J. Berry, J. Chem. Phys. 59, 6229 (1973).

[12]N. C. Blais and D. G. Truhlar, J. Chem. Phys. 58, 1090 (1973).

[13]T. P. Schaefer, P. E. Siska, J. M. Parson, F. P. Tully, Y. C. Wong, and Y. T. Lee, J. Chem. Phys. 53, 3385 (1970). See also Ref. 10.

[14]A. Ding, L. Kirsch, D. Perry, J. Polanyi, and J. Schreiber, Discuss. Faraday Soc. 55, 252 (1973).

[15]G. C. Schatz and A. Kuppermann (unpublished calculations).

[16]G. C. Schatz and A. Kuppermann, J. Chem. Phys. 59, 964 (1973).

[17]R. D. Levine and S.-F. Wu, Chem. Phys. Lett. 11, 557 (1971).

[18]J. R. Stine and R. A. Marcus, Chem. Phys. Lett. 29, 575 (1974). This work appeared in print after the present paper was submitted for publication. All references to it were incorporated subsequently, at the time some revisions suggested by the referee were made.

[19]J. D. Duff and D. G. Truhlar, Chem. Phys. 4, 1 (1974).

[20]Note that for these calculations, a slightly different value of β(HF) was used (2.2087 $Å^{-1}$) than in Paper I (2.2187 $Å^{-1}$).

[21]A. Persky, J. Chem. Phys. 59, 5578 (1973).

[22]M. Baer, U. Halavee, and A. Persky, J. Chem. Phys. 61, 4362 (1974).

[23]Recent three dimensional calculations on the H + H_2 reaction indicate that the attenuation of resonance effects in going from 1D to 3D is not severe [G. C. Schaty and Aron Kuppermann (to be published)].